

Retraction

Retracted: Research on Improved Droop Control Strategy of Microsource Inverter Based on Internet of Things

Security and Communication Networks

Received 25 July 2023; Accepted 25 July 2023; Published 26 July 2023

Copyright © 2023 Security and Communication Networks. This is an open access article distributed under the Creative Commons Attribution License, which permits unrestricted use, distribution, and reproduction in any medium, provided the original work is properly cited.

This article has been retracted by Hindawi following an investigation undertaken by the publisher [1]. This investigation has uncovered evidence of one or more of the following indicators of systematic manipulation of the publication process:

- (1) Discrepancies in scope
- (2) Discrepancies in the description of the research reported
- (3) Discrepancies between the availability of data and the research described
- (4) Inappropriate citations
- (5) Incoherent, meaningless and/or irrelevant content included in the article
- (6) Peer-review manipulation

The presence of these indicators undermines our confidence in the integrity of the article's content and we cannot, therefore, vouch for its reliability. Please note that this notice is intended solely to alert readers that the content of this article is unreliable. We have not investigated whether authors were aware of or involved in the systematic manipulation of the publication process.

Wiley and Hindawi regrets that the usual quality checks did not identify these issues before publication and have since put additional measures in place to safeguard research integrity.

We wish to credit our own Research Integrity and Research Publishing teams and anonymous and named external researchers and research integrity experts for contributing to this investigation.

The corresponding author, as the representative of all authors, has been given the opportunity to register their agreement or disagreement to this retraction. We have kept a record of any response received.

References

- [1] D. Bai, T. Zhang, and Z. Yang, "Research on Improved Droop Control Strategy of Microsource Inverter Based on Internet of Things," *Security and Communication Networks*, vol. 2021, Article ID 5043623, 8 pages, 2021.

Research Article

Research on Improved Droop Control Strategy of Microsource Inverter Based on Internet of Things

Di Bai^{1,2}, Tieyan Zhang,¹ and Zheng Yang³

¹College of Information and Electrical Engineering, Shenyang Agricultural University, Shenyang, Liaoning 110866, China

²College of Electric Power, Shenyang Institute of Engineering, Shenyang, Liaoning 110136, China

³College of Information, Shenyang Institute of Engineering, Shenyang, Liaoning 110136, China

Correspondence should be addressed to Di Bai; baidi@sie.edu.cn

Received 26 October 2021; Revised 12 November 2021; Accepted 17 November 2021; Published 1 December 2021

Academic Editor: Jian Su

Copyright © 2021 Di Bai et al. This is an open access article distributed under the Creative Commons Attribution License, which permits unrestricted use, distribution, and reproduction in any medium, provided the original work is properly cited.

Microgrid connects the distributed power supply with the assistance of power electronic devices. Power electronic devices, especially in the inversion link, play a crucial role in the access of distributed power to microgrid. Whether in grid-connected mode or island mode, the control method of inverters is related to the stable operation of distributed power supply and plays an important role in the control strategy of microgrid. In this paper, by adding the drop control of controllable virtual impedance, the power coupling problem caused by resistive line impedance is reduced, and virtual impedance key points such as voltage feedback and frequency compensation are added. By optimizing the power reference value, the parallel operation stability of the control strategy is improved. The experimental results show that the proposed method improves not only the stability of the system and the power quality but also the accuracy of reactive power distribution.

1. Introduction

At present, droop control is widely used in microgrids, especially in microgrids with point-to-point control [1]. However, the impedance of distribution lines in microgrid may be due to the presence of isolated transformers and power electronic converters with nonpure resistance characteristics in the lines. The traditional sag control may result in slowing down the adjustment speed of the system, even destroying the system stability in serious cases [2]. Scholars at home and abroad have carried out a series of studies on this, designed the inverter base wave and harmonic cross-over droop controller, which can effectively suppress the voltage harmonics and rationally distribute the power in the base wave and harmonic domain according to the capacity, thereby improving the power allocation accuracy when the inverters are in parallel [3, 4].

To improve the accuracy of load distribution, voltage amplitude feedback is added on the basis of traditional droop control, which improves the accuracy of load distribution. However, this method requires a large reactive

droop coefficient, which is not conducive to the stability of the system [5]. The virtual impedance technology is introduced into the traditional droop control. Virtual reactance is added to the output side of the distributed generation inverter to make its output impedance inductive, and then, the Q/V curve is modified to improve the accuracy of reactive power distribution [6]. However, the introduction of virtual impedance will reduce the voltage of the system and adversely affect the output voltage quality [7]. The improved control based on dynamic virtual impedance is adopted to adjust the virtual impedance value adaptively, reduce the line voltage drop, and suppress the reactive power cycle [8]. The reactive power deviation is added to the P/f droop control as a disturbance, and then, the disturbance is used to adjust the Q/V droop control of each micropower source to reduce the reactive power allocation error, but this method will cause the fluctuation of system frequency and have adverse effects on power quality [9].

The virtual impedance method is proposed to reduce the impedance difference of each microsource line, to improve the distribution accuracy of microsource reactive load, but

this problem cannot be fundamentally solved. Therefore, on the premise of not affecting the power quality and the stability of the microgrid system, seeking an effective method to improve the accuracy of reactive power distribution in microgrid has become a hotspot of microgrid research.

2. Principle Analysis of the Traditional Droop Control Method

Droop control is a kind of reverse regulation principle. Before reverse regulation, the output voltage amplitude and frequency command value should be obtained through droop characteristic. According to the power frequency static characteristics of the generator set, the distribution of active and reactive power can meet the reasonable requirements. By using the inverse fine-tuning parameters, the inverter output voltage amplitude is reasonable and the frequency is stable, to realize the stable operation of DG parallel system of microgrid [10]. The frequency droop characteristic curve similar to the traditional generator is selected as the control mode of microsource, that is, the stable frequency and voltage are obtained by P - F droop control and q - u droop control, respectively. This control method can control the active power and reactive power of microsource output in microgrid separately without communication and coordination between units. It achieves the goal of microsource plug and play and peer-to-peer control, ensures the unity of power balance and frequency in the microgrid under isolated island, and has the characteristics of simple and reliable.

In the initial operation state of the microgrid system, the system frequency and inverter are connected to the grid, the output active power is f_0 and p_0 , respectively, and the output reactive power is Q_0 , as shown in Figure 1; the voltage at the cross node of the grid-connected inverter and AC bus is U_0 . The increase of voltage and power output in microgrid will lead to the increase of access power, and the output power of power supply will be insufficient, resulting in the decrease of frequency. The droop coefficient will be obtained to help the distributed generation increase the active power output, and the system frequency and load power consumption will decrease synchronously [11]. Finally, a new balance point C is determined, which is formed by the interaction between distributed generation and load to achieve a stable power balance, namely, f - P control [12]. Another case is that the reactive power is reduced, the system voltage is reduced, and the droop characteristic causes the distributed generation to increase the reactive power output. With the decrease of voltage, the load synchronously changes to the equilibrium point and the stable operation position at C, namely, U - Q control [13].

The voltage level of microgrid is low and the ratio of resistance to inductance is relatively high [14]. When the inverter is connected to the AC bus, the resistance will change with the distance, and the line resistance will increase with the distance. Droop control causes the voltage and frequency of the conventional low-voltage microgrid

inverter to be affected, which cannot meet the system requirements [15].

Droop control is an output power control method which adjusts the frequency and amplitude of voltage through f - P and U - Q . It can also be controlled by P - f and Q - U . By adjusting the output power, the frequency and amplitude of the control voltage can be achieved.

The P - f and Q - U equations are as follows:

$$\begin{cases} p = p_0 + K_f(f_0 - f), \\ Q = Q_0 + K_U(U_0 - U). \end{cases} \quad (1)$$

The f - P and U - Q equations are as follows:

$$\begin{cases} f = f_0 + K_P(P_0 - P), \\ U = U_0 + K_Q(Q_0 - Q). \end{cases} \quad (2)$$

The droop control in Figure 2 is based on f - P and U - Q , the outer-loop structure droop control mode; the dotted line part is internal power control and the other part is external droop control. The reference data are obtained from the calculation results of formulas (1) and (2), and the frequency and voltage amplitude, active power, and reactive power are assigned. The parameter value of droop factor in the figure is distributed by the active power and reactive power of the distributed generation. The inner loop is controlled by the power and provides the reference data of current control, which constitutes two parts of the outer-loop controller. Among them, the low-pass filter $1/1 + sT$ and the time filter $T = [P/P \cdot (SOC_{pb} - SOC_{sc}) + 0.5] \cdot T_0$. In the outer-loop control section, the frequency and voltage signals received by the controller for the output of the inverter are converted into reference values for the power of the outer loop. The reference values of the inner-loop current are obtained by adjusting the PI regulator according to the difference between the power reference values and the actual measured values by the outer-loop controller. Based on this reference value, the controller adjusts the power output by controlling the current output of the inverter and finally adjusts the voltage and frequency in the power network to approximate the given reference value.

According to the droop control principle, the grid-connected inverter detects the AC bus of the microgrid system, obtains the voltage and current, and calculates the active power and reactive power. As shown in Figure 3, the reference data are obtained from the above calculation results, and the frequency and voltage amplitude are assigned according to the droop characteristics. The droop control strategy uses the control signal to adjust the distributed generation and control the inverter state. As shown in the figure, the output signal is P_{md} and P_{mq} , and the DQ axis component is adjusted to adjust the system voltage amplitude output of active power and reactive power. Because the grid-connected inverter is prone to voltage fluctuation when the load nonlinear ratio is too large or asymmetric, in order to select the droop control strategy, the voltage fluctuation must be reduced, and the method of increasing voltage should be used in the strategy.

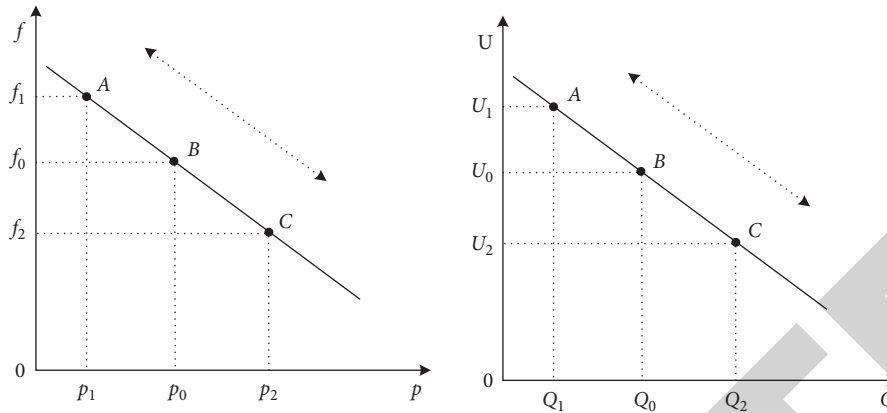


FIGURE 1: Schematic diagram of droop control.

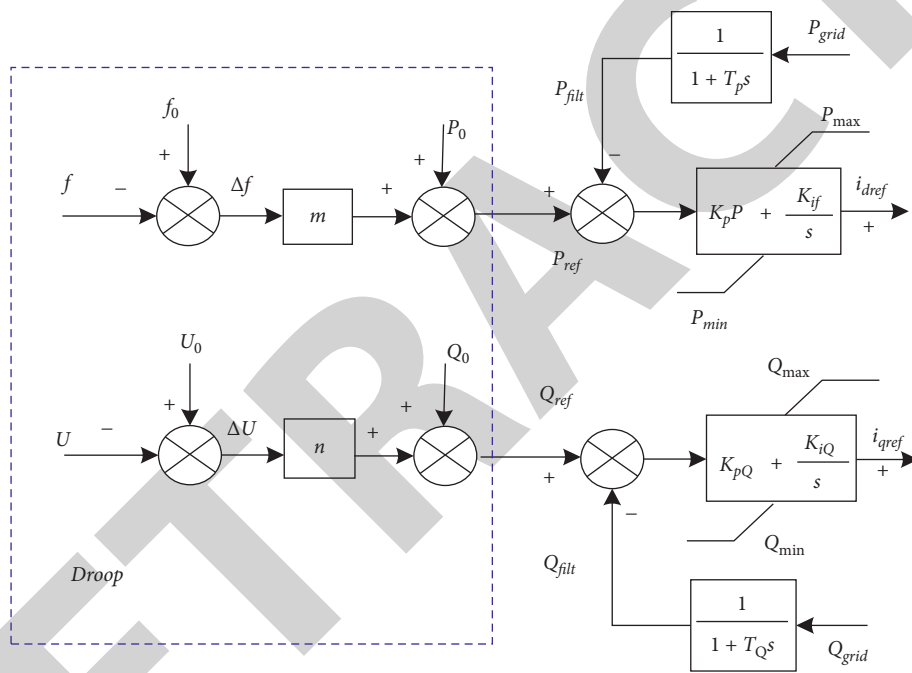


FIGURE 2: Typical structure of the outer-loop controller with droop control mode of f - P and U - Q .

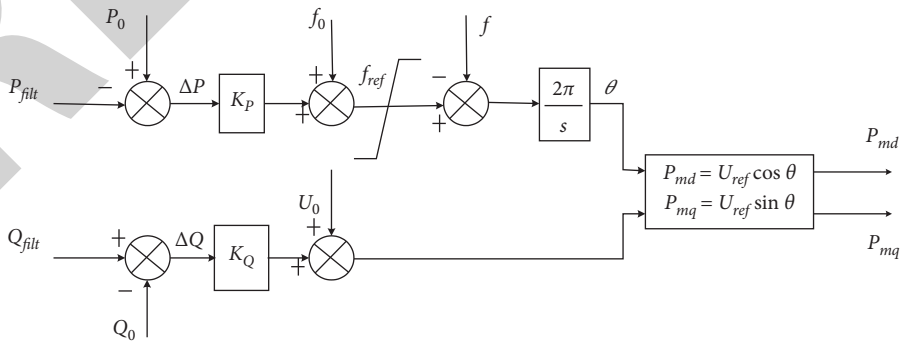


FIGURE 3: Typical structure of outer-loop controller with P - f and Q - U droop control mode.

3. Improved Droop Control Strategy

3.1. Traditional Droop Control Strategy of the Inverter. The inverter needs to use the on and off of the main switch device to obtain three-phase AC output and adopts three-phase bridge six-switch structure. As shown in Figure 4, the nominal AC voltage of the microgrid is 380 V, and the interface voltage is 800 V when designing DC bus. The three-phase bridge six-switch inverter needs power electronic devices, control circuit, drive circuit, and power supply. Because the three-phase bridge six switch compared with the long converter, there is no imbalance problem, so this paper designs and uses this switch.

When the microgrid load is assumed to be linear, the complex phase circuit model of the microgrid includes two interfaces of the microgrid inverter operating in voltage control mode, as shown in Figure 5. It is assumed that points 1 and 2 represent the port of the microsource interface inverter connected to the microgrid, and point 0 represents the equivalent common connection point connecting other microsource inverter interfaces, energy storage devices, and loads in the microgrid.

In this paper, assuming linear load as the premise, the model contains two microgrid inverter interfaces, which are voltage control modes. The complex phase circuit model of the microgrid is constructed, as shown in Figure 5. The micropower supply uses two points A and B as ports to connect the micropower interface, inverter, and microgrid and point C as the common connection. In the microgrid, several microsources and energy storage devices are connected, respectively, and the loads are connected at the same time.

$E_i \angle \theta_i$: it is output voltage phasor; the equipment is the interface inverter.

$V = \angle 0^\circ$: it is voltage phasor, location of the common connection point.

$Z_i \angle \varphi_i = R_i + jX_i$: it is between the microsource inverter i and the common connection point C; the equivalent line

complex impedance, line resistance, and line reactance are, respectively, R_i and X_i .

As shown in Figure 5, the voltage of point C is obtained. There are several interfaces of microsource inverter, which are connected to point C. The evaluation formula of point C voltage is as follows:

$$\dot{V} = \sum_{j=1}^n \left(1 - \frac{Z_j}{Z_j + Z_{sj}} \right). \quad (3)$$

If the impedance in the circuit is mainly inductive, $\phi_{Zi} \approx 90^\circ$ and $Z \approx jX$, there is

$$\begin{cases} p_i = \frac{V_i V_L \theta_{iL}}{X_i} \\ q_i = \frac{V_L}{X_i} (V_i - V_L) \end{cases} \Rightarrow \begin{cases} \omega_i = \omega^* - k_{pi} (p_i - p_i^*), \\ V_i = V^* - k_{qi} (q_i - q_i^*), \end{cases} \quad (4)$$

where p_i is the active power output by the inverter i , q_i is the reactive power output by the inverter i , ϕ_{Zi} is the phase angle of the line impedance, V_i is the output voltage value of the inverter, V_L is the voltage amplitude at the PCC point, $\theta_{iL} = \theta_i - \theta_L$ is the phase difference, θ_i is the output voltage phase angle of the inverter, and θ_L is the PCC point voltage phase angle. When the line impedance is mainly resistive, $\phi_{Zi} \approx 0^\circ$ and $Z \approx R$:

$$\begin{cases} p_i = \frac{V_L}{R_i} (V_i - V_L) \\ q_i = \frac{V_i V_L \theta_{iL}}{R_i} \end{cases} \Rightarrow \begin{cases} \omega_i = \omega^* - k_{qi} (q_i - q_i^*), \\ V_i = V^* - k_{pi} (p_i - p_i^*). \end{cases} \quad (5)$$

When the impedance of the line is mainly inductive, $0^\circ < \phi_{Zi} < 90^\circ$ and $Z = jX + R$, there is

$$\begin{cases} \frac{V_L (V_i - V_L)}{Z_n} \cos \phi_{Zi} + \frac{V_i V_L \theta_{iL}}{Z_n} \sin \phi_{Zi} \\ \frac{V_L (V_i - V_L)}{Z_i} \sin \phi_{Zi} - \frac{V_i V_L \theta_{iL}}{Z_n} \cos \phi_{Zi} \end{cases} \Rightarrow \begin{cases} \omega_i = \omega^* - k_{pi} \left[\frac{X}{Z} (p_i - p_i^*) - \frac{R}{Z} (q_i - q_i^*) \right], \\ V_i = V^* - k_{qi} \left[\frac{R}{Z} (p_i - p_i^*) + \frac{X}{Z} (q_i - q_i^*) \right]. \end{cases} \quad (6)$$

The output voltage of each inverter and the parameters of line impedance are the factors that affect the voltage amplitude of point B. When the line impedance remains unchanged, the zero point voltage can be obtained by weighting the output voltage of the inverter and the line impedance. When the weight is $Z_{sj}/Z_j + Z_{sj}$, the active power and reactive power output of micro source i can be obtained as follows:

$$\begin{aligned} P_i &= \frac{1}{Z_i} \left[(E_i^2 - VE_i \cos \theta_i) \cos \phi_i + VE_i \sin \theta_i \sin \phi_i \right], \\ Q_i &= \frac{1}{Z_i} \left[(E_i^2 - VE_i \cos \theta_i) \sin \phi_i - VE_i \sin \theta_i \cos \phi_i \right], \end{aligned} \quad (7)$$

where E_i is the interface voltage of the energy storage inverter. It can be seen from equation (7) that the output voltage amplitude, voltage phase angle, line reactance, and

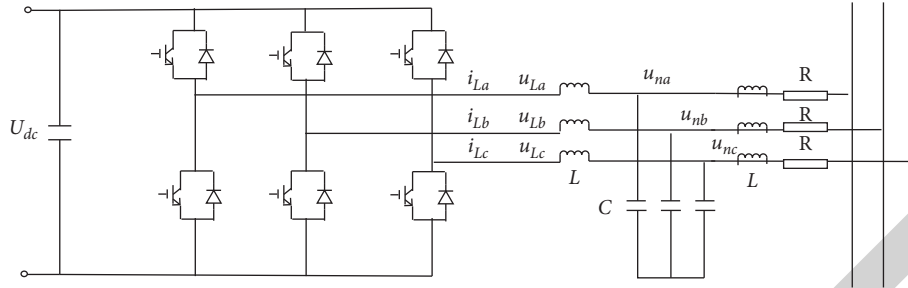


FIGURE 4: Inverter circuit.

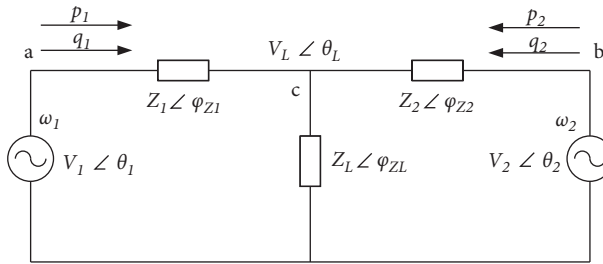


FIGURE 5: Simplified model of a microgrid system with dual microsources.

resistance of each micropower supply will determine the output active and reactive power. When the ratio of reactance to line resistance is greater than 3, the sine function $\sin \phi_I$ is close to 1 and the cosine function $\cos \phi_i$ is close to 0. Because the resistance in each distribution line is greater than reactance, the power expression of micropower inverters (7) can be simplified to

$$P_i \approx \frac{E_i(E_i - V)}{Z_i}, \quad (8)$$

$$Q_i \approx \frac{E_i V}{Z_i} \theta_i.$$

3.2. Effect of Line Impedance Inequality on Droop Control.

In low-voltage microgrid, the difference of the distance between PCC points and each interface inverter results in different length of line from PCC point to each inverter, i.e., different line impedance, which is caused by the spatial distribution of each interface inverter. The traditional linkless down control has different impedances, which can cause problems for the active and reactive output of the inverters. Regardless of the transient stability of the output voltage of a single inverter, the influence of line impedance on the active power output of the inverter is analyzed, and the closed-loop control mathematical model of the inverter is obtained by combining the virtual active power expression of the inverter output:

$$P_{xi} = \frac{E_i V \theta_i}{|Z_i|}, \quad (9)$$

$$\omega_i = \omega^* - m_i P_{xi},$$

$$\theta_i = \int (\omega_i - \omega_0) dt.$$

Where type ω_0 is the no-load output angular frequency of the inverter in rad/s and m_i represents the inverter reactive power droop coefficient. Droop coefficient of the inverter is inversely proportional to its capacity.

From equation (9), the difference between the bus voltage frequency and the no-load frequency of the input PCC connection is obtained by using the virtual active power output from the micropower inverter i to get the closed transfer function:

$$\frac{P_{xi}}{\omega^*(s) - \omega_0(s)} = \frac{E_i V}{s|Z_i| + E_i V m_i}. \quad (10)$$

When the micronetwork is running stably, the output voltage and common voltage of the inverter are regarded as constants, and the equation can be solved, that is, the virtual reactive power output of the inverter is

$$Q_{xi} = \frac{b - \sqrt{b^2 - 4n_i^2 E^* (E^* - V)}}{2n_i^2}. \quad (11)$$

According to equation (11), the droop coefficient n_i and the impedance modulus $|Z_i|$ of distribution line will affect the output virtual reactive power of the inverter. The results show that $dQ_{xi}/d(|Z_i|) < 0$ is a monotonic decreasing function of $Q_{xi} = f(|Z_i|)$, and the output virtual reactive power decreases with the increase of impedance modulus. The condition in which the reactance and resistance of the line are inversely proportional to the output virtual reactive power of the inverter is that the droop control coefficient should be a fixed value; the output virtual reactive power of the inverter decreases with the increase of droop coefficient when the line reactance or line resistance is a fixed value.

3.3. *Improvement of Droop Control Based on Virtual Impedance.* The actual output power of the inverter with the same capacity can be calculated by equation (11), which can be obtained according to the droop control principle of virtual power:

$$\begin{aligned} \begin{bmatrix} P_1 \\ Q_1 \end{bmatrix} &= \begin{bmatrix} \sin \phi_1 - \cos \phi_1 \\ \cos \phi_1 \sin \phi_1 \end{bmatrix}^{-1} \begin{bmatrix} P_{x1} \\ Q_{x1} \end{bmatrix} \\ &= \begin{bmatrix} \sin \phi_1 \cos \phi_1 \\ -\cos \phi_1 \sin \phi_1 \end{bmatrix} \begin{bmatrix} P_{x1} \\ Q_{x1} \end{bmatrix}. \end{aligned} \quad (12)$$

It can be seen from equation (12) that the conversion matrix between the virtual power and the actual power is a nonsingular matrix, so the unique solution can be obtained. To share the output power of each inverter equally, each inverter should have the same actual power P_1 and Q_1 . In this way, the transformation matrix of the impedance ratio of each line should have the same inverse matrix, and each inverter should have the same active power P_{x1} and reactive power Q_{x1} .

It has been analyzed that because of the uncertainty of the line length from PCC contact to the inverter, the influence of line impedance on the output active power of the inverter must be considered. To solve the problem of unbalanced power loss, we can use the method of compensating the line impedance to make the actual impedance equal. The variable virtual impedance compensation line impedance shown in formula (13) is added to the control of the interface inverter of the microgrid inverter:

$$|Z_1^*| = kQ_{x1}. \quad (13)$$

According to the analysis in the previous section, the output virtual reactive power of the micro power inverter is inversely proportional to the line impedance mode. To reduce the serious power output imbalance of the micropower inverter and make the line equivalent impedance tend to be equal, a variable virtual impedance control strategy can be introduced into the interface inverter. According to formula (13), the larger the virtual impedance is, because the virtual reactive power is proportional to the virtual impedance, the greater the virtual reactive power is. The block diagram is shown in Figure 6.

The expression of virtual impedance is

$$\begin{aligned} \Delta u_{od} &= R_x i_{od} - \omega L_x i_{oq} + L_x \dot{i}_{od}, \\ \Delta u_{oq} &= R_x i_{oq} + \omega L_x i_{od} + L_x \dot{i}_{oq}. \end{aligned} \quad (14)$$

4. Simulation Analysis of Variable Virtual Impedance Droop Control

The simulation model is built according to the variable virtual impedance droop control block diagram shown in Figure 6, and the simulation parameters are set as follows. The transmission line impedance between photovoltaic interface inverter 1 and microgrid public connection point is $R1 = 0.5 \Omega$ and $L1 = 0.001H$, the transmission line impedance

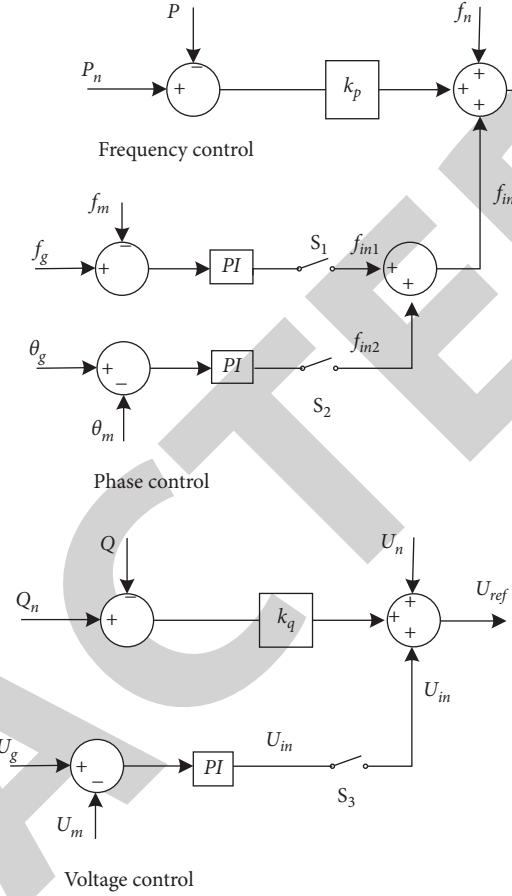


FIGURE 6: Synchronous control structure for grid connection.

between public connection points of photovoltaic interface inverter 2 microgrid is $R2 = 0.2 \Omega$ and $L2 = 0.0005H$, public load within islands operating microgrid system is $Rload = 25 \Omega$ and $Lload = 0.02H$, the simulation results show that the active power droop coefficient is 0.01 and the reactive power droop coefficient is 0.28, the inverter uses traditional power droop control (without virtual impedance), and the actual output active power and reactive power simulation waveforms of the inverter are shown in Figure 7.

Under the same simulation parameters, when the variable virtual impedance is added to the traditional virtual power droop control, the actual output active power and reactive power simulation waveforms of the microsource inverter are shown in Figure 8.

Compared with the simulated waveforms of the actual power, in Figures 7 and 8, it is found that the virtual power droop control with variable virtual impedance not only achieves the virtual power sharing of the photovoltaic interface inverters but also reduces the actual output active power difference of the two photovoltaic interface inverters by 4/5 and the relative power difference by 83%. After adjusting the virtual power control, the actual active power of the two energy routers is nearly 1/5 of the original, and the relative value of the power difference is reduced to the traditional 15%. The simulation results show that the virtual power droop control with variable virtual impedance achieves the virtual power the virtual power sag control with virtual impedance which can significantly

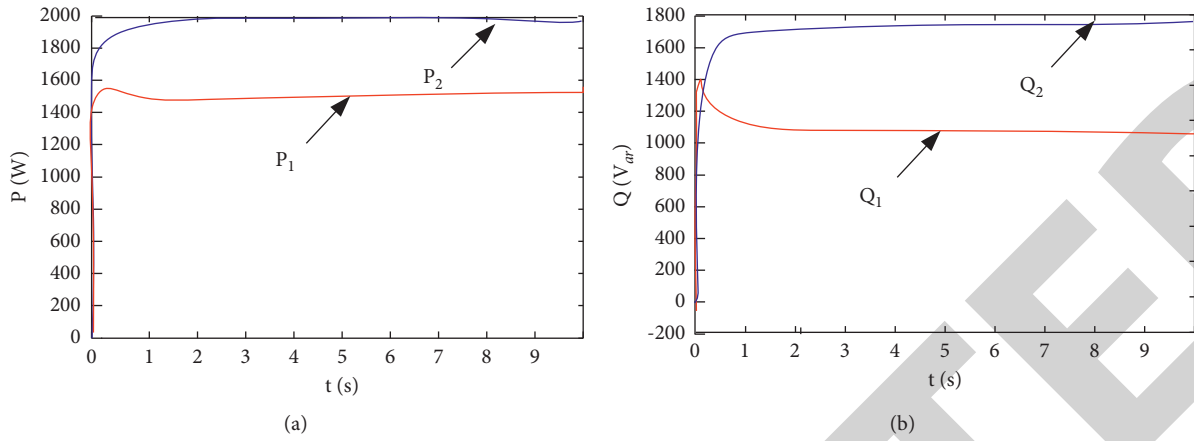


FIGURE 7: The output true power waveforms without virtual impedance.

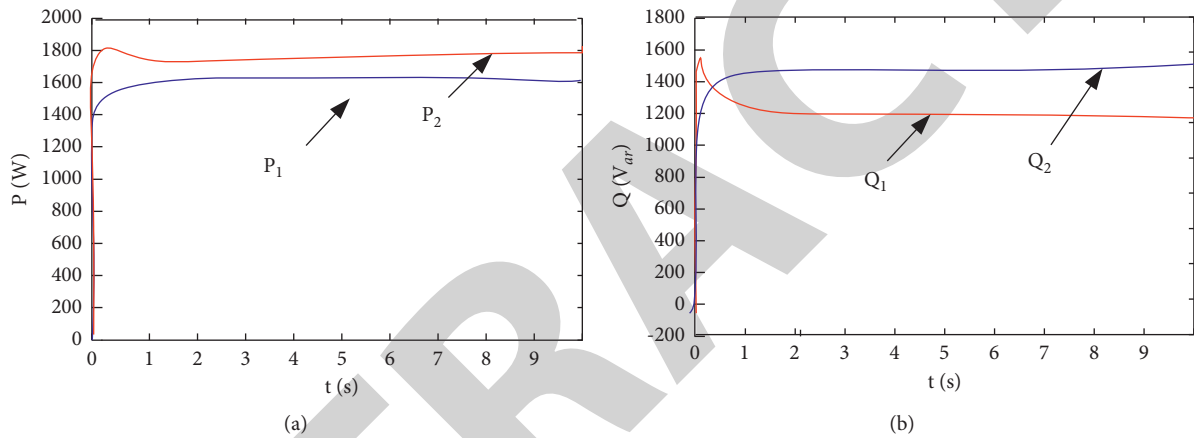


FIGURE 8: The output true power waveforms with variable virtual impedance control.

improve the uneven output power of photovoltaic interface inverters due to different transmission line impedance. Through the above simulation analysis, compared with the traditional droop control and the virtual power droop control of virtual impedance proposed in this paper, it can be found that the improved droop control can improve the system stability of microgrid in off-grid operation and realize average power distribution.

5. Conclusion

By analyzing the characteristics of traditional droop control, this paper expounds the influence of various types of line impedance on the output power balance of the inverter and the stable operation of microgrid; the basic principle of virtual impedance is studied. The control strategy of virtual impedance is introduced by observing the change of system output characteristics. The power coupling problem caused by the impedance of the resistive line is weakened by controllable virtual impedance. The key points of virtual impedance such as voltage feedback and frequency compensation are added. The grid-connected operation stability of the control strategy is improved by optimizing the power reference value, improving the power quality of microgrid. The virtual power droop

control with virtual impedance can significantly improve the uneven output power of photovoltaic interface inverter caused by different transmission line impedance. A simulation model is used to verify the virtual power sag control with virtual impedance, compared with the traditional method, which improves the system stability and achieves the average power distribution of the microgrid connected to the power grid when it is running offline.

Data Availability

The simulation experiment data used to support the findings of this study are available from the corresponding author upon request.

Conflicts of Interest

The authors declare that there are no conflicts of interest regarding the publication of this paper.

Acknowledgments

This work was supported in part by the Liaoning Provincial Department of education (Grant no. JL-1905).

References

- [1] Y. Krim, S. Krim, and M. F. Mimouni, "Control of a wind farm connected to the grid at a frequency and variable voltage," *International Journal of Renewable Energy Resources*, vol. 6, no. 3, pp. 747–758, 2016.
- [2] A. B. Moreira, T. A. S. Barros, V. S. C. Teixeira, and E. Ruppert, "Power control for wind power generation and current harmonic filtering with doubly fed induction generator," *Renewable Energy*, vol. 107, pp. 181–193, 2017.
- [3] Z. Liu, L. Lang, L. Li, Y. Zhao, and L. Shi, "Evolutionary game analysis on the recycling strategy of household medical device enterprises under government dynamic rewards and punishments," *Mathematical Biosciences and Engineering: MBE*, vol. 18, no. 5, pp. 6434–6451, 2021.
- [4] S. Qiuye, F. Ruyi, L. Yushuai, H. Bonan, and M. Dazhong, "A distributed double-consensus algorithm for residential wenergy," *IEEE transactions on industrial informatics*, vol. 15, no. 8, pp. 4830–4842, 2019.
- [5] X. Ding, R. Yao, X. Zhai, C. Li, and H. Dong, "An adaptive compensation droop control strategy for reactive power sharing in islanded microgrid," *Electrical Engineering*, vol. 102, no. 1, pp. 267–278, 2020.
- [6] R.-J. Wai, Q.-Q. Zhang, and Y. Wang, "A novel voltage stabilization and power sharing control method based on virtual complex impedance for an off-grid microgrid," *IEEE Transactions on Power Electronics*, vol. 34, no. 2, pp. 1863–1880, 2019.
- [7] K. K. Preethi, S. Chenrayan, P. Marimuthu, L. C. Woo, and V. Kumaran, "One dimensional vanadium boron-oxyfluoride nanostructures for lithium storage systems," *Materials Letters*, vol. 293, p. 2932, 2021.
- [8] Y. Sun, X. Hou, J. Yang, H. Han, M. Su, and J. M. Guerrero, "New perspectives on droop control in ac microgrid," *IEEE Transactions on Industrial Electronics*, vol. 64, no. 7, pp. 5741–5745, 2017.
- [9] A. Milczarek, M. Malinowski, and J. M. Guerrero, "Reactive power management in islanded microgrid-proportional power sharing in hierarchical droop control," *IEEE Transactions on Smart Grid*, vol. 6, no. 4, pp. 1631–1638, 2017.
- [10] R. Irnawan, F. F. D. Silva, C. L. Bak, A. M. Lindefelt, and A. Alefragkis, "A droop line tracking control for multi-terminal VSC-HVDC transmission system," *Electric Power Systems Research*, vol. 17, 2020.
- [11] G. Vikash, A. Ghosh, P. K. Anup, and R. Shubhobrata, "Implementation and comparison of droop control, virtual synchronous machine, and virtual oscillator control for parallel inverters in standalone microgrid," *International Transactions on Electrical Energy Systems*, vol. 31, no. 5, 2021.
- [12] R. Chandran, S. R. Kumar, and N. Gayathri, "Genetic algorithm-based tabu search for optimal energy-aware allocation of data center resources," *Soft Computing*, vol. 24, no. 7, pp. 1–14, 2020.
- [13] T. Zhou, W. Wu, L. Peng et al., "Evaluation of urban bus service reliability on variable time horizons using a hybrid deep learning method," *Reliability Engineering & System Safety*, vol. 217, Article ID 108090, 2020.
- [14] W. Shu, K. Cai, and N. N. Xiong, "Research on strong agile response task scheduling optimization enhancement with optimal resource usage in green cloud computing," *Future Generation Computer Systems*, vol. 124, pp. 12–20, 2021.
- [15] W. W, X. Xia, M. Wozniak, X. Fan, R. Damaševičius, and Y. Li, "Multi-sink distributed power control algorithm for cyber-physical-systems in coal mine tunnels," *Computer Networks*, vol. 161, pp. 210–219, 2019.